Equilibrium dynamics of the sine-Gordon chain: A molecular-dynamics study

W. C. Kerr
Department of Physics, Wake Forest University, Winston-Salem, North Carolina 27109 and Argonne National Laboratory, Argonne, Illinois 60439

D. Baeriswyl
RCA Laboratories Ltd., Badenerstrasse 569, CH-8048 Zurich, Switzerland

A. R. Bishop
Theoretical Division and Center for Nonlinear Studies, University of California, Los Alamos National Laboratory, Los Alamos, New Mexico 87545
(Received 6 July 1981)

Results of a molecular-dynamics study of the discrete sine-Gordon (SG) chain are reported, emphasizing ϕ-ϕ, sinϕ-sinϕ, and cosϕ-cosϕ dynamic correlation functions (ϕ is the SG field variable). Correlations at the temperature $k_BT \simeq 0.29E_K$ (E_K is the continuum SG kink-soliton energy) are interpreted in terms of elementary linear and nonlinear modes—kinks, breathers, single-, and multiphonons. The validity of "ideal-gas" approximations is assessed and corrections from lattice discreteness and mode-mode interactions are discussed. Finally, the relevance of our results to planar ferromagnetic chains (e.g., $CsNiF_3$) in an easy-plane applied magnetic field is assessed.

I. INTRODUCTION

In this paper we describe and interpret results from our molecular dynamics (MD) simulation of the sine-Gordon (SG) chain. This is a one-dimensional system where each particle interacts with its neighbors through harmonic forces and also moves in an externally imposed sinusoidal potential which can be thought of as arising from a rigid background lattice. The equations of motion for the system are

$$M\ddot{U}_n = C(U_{n+1} - 2U_n + U_{n-1}) - \frac{2\pi}{a} A \sin\left[\frac{2\pi}{a} U_n\right] , \quad n = 1, \ldots, N . \tag{1}$$

The total number of particles is N each with mass M, the displacement of the nth particle from its equilibrium position is U_n, and the lattice constant is a. C and A are constants giving the strengths of the linear and nonlinear forces, respectively.

These equations of motion are integrated by an algorithm due to Beeman,[1] which has previously been used in a study of structural phase transitions.[2] The total energy is a constant of the motion in this integration scheme. This technique should be contrasted with the coupled Langevin equation scheme of Schneider and Stoll,[3] which keeps the temperature constant, and our results for the SG chain may be considered complementary to theirs. The results reported here are limited to a single temperature T (see below).

Our primary aim is to understand the dynamic structure factors

$$S_{XX}(q,\omega) = N^{-1} \int_{-\infty}^{\infty} dt\, e^{i\omega t} \langle X(q,t) X(-q,0) \rangle , \tag{2}$$

where the wave-vector-dependent fluctuation is defined by

$$X(q,t) = \sum_{n=1}^{N} e^{-iq(n-1)a} X_n(t) . \tag{3}$$

The three local variables for which we present results are (i) the displacement (U), or more precisely its phase (ϕ) relative to the periodic potential

$$X_n(t) \to \phi_n(t) = \frac{2\pi}{a} U_n(t) . \tag{4}$$

(ii) the sine (s) of this phase variable

$$X_n(t) \to s_n(t) = \sin\left[\frac{2\pi}{a} U_n(t)\right] , \tag{5}$$

and (iii), the fluctuation of the cosine (c) of the phase variable

$$X_n(t) \to c_n(t) = \cos\left[\frac{2\pi}{a} U_n(t)\right] - \left\langle \cos\left[\frac{2\pi}{a} U_n(t)\right] \right\rangle . \tag{6}$$

 ©1981 The American Physical Society

The wave vectors q are determined from the periodic boundary conditions in the usual way: $q=2\pi m/(Na)$, where m is an integer. We will frequently use the dimensionless wave vector $\tilde{q}\equiv qa/\pi=2m/N$.

We try to interpret results in terms of the natural elementary modes of the SG equation (1), namely *kinks, breathers, and phonons* (magnons).[3–6] Appealing, but intrinsically simplistic "ideal gas" approximations have been widely used in the literature[4,5] and it is now important to begin to quantify these. An important advantage of the MD simulation is that the integrated weight $\int S(q,\omega)d\omega$ can be examined separately for "high"- and "low"-frequency regimes, and we will present results for each of these two regimes. This information is not available from transfer integral schemes[6] without phenomenological approximations, and as we shall see, the total and partial integrated weights can have rather different q dependence. Since "central peaks" (i.e., low-frequency components) have frequently[4] been attributed to kinks, it is important to understand this probe of nonlinear modes more quantitatively. In particular, interpretation of neutron scattering data in easy-plane Heisenberg magnetic chains [e.g., $CsNiF_3$ or $(CD_3)_4NMnCl_3$(TMMC)] has so far depended heavily on simple kink theories to explain anomalous central peaks.[5–8] Although serious questions remain about the validity of a pure SG description (particularly regarding quantum effects,[9] damping, and the importance of nonlinear out-of-plane spin motions[10–12]), we will see that some qualitative trends may help to explain the notable partial successes of ideal kink-gas theory data fits. Having in mind $CsNiF_3$ in the presence of a 5-kG in-plane magnetic field,[5,7] we have chosen the following parameters for Eq. (1): $M=1$, $A=1$, $a=2\pi$, and $C=29.22$ (see also Ref. 3). For these parameter values the kink width is approximately $10a$. For many, but *not* all (see below) properties this validates a continuum SG approximation to (1), as is frequently assumed[4–8]: Equation (1) then becomes

$$c_0^2\phi_{xx}-\phi_{tt}=\omega_0^2\sin\phi\ , \tag{7}$$

where

$$c_0^2\equiv Ca^2/M$$

and

$$\omega_0^2=4\pi^2A/(Ma^2)\ .$$

For the numerical integration of Eq. (1), the dimensionless variable $\omega_0 t$ was used, and these equations were integrated for 50 000 time steps using a step size of $\Delta(\omega_0 t)=0.08$.

II. PREDICTIONS OF IDEAL GAS PHENOMENOLOGY

The structure factor predicted from an *ideal* relativistic [cf. Eq. (7)] gas of SG *kinks*, $S_{XX}^K(q,\omega)$, is by now well documented[3,4,13]:

$$S_{XX}^K(q,\omega)=\frac{n_K(T)}{2\pi q}P\left[\frac{\omega}{q}\right]\gamma^{-2}\left[\frac{\omega}{q}\right]\left|f_X^K\left[q\gamma^{-1}\left[\frac{\omega}{q}\right]\right]\right|^2 \tag{8}$$

with $\gamma(v)\equiv(1-v^2/c_0^2)^{-1/2}$, n_K the kink (plus antikink) density, and $P(v)$ the ideal relativistic gas velocity (v) distribution,

$$P(v)=[2c_0K_1(\alpha)]^{-1}\gamma^3(v)\exp[-\alpha\gamma(v)]\ ,\qquad \alpha=E_K^{(0)}/k_BT\ . \tag{9}$$

(K_1 is a modified Bessel function.)

The functions f_X^K are "form factors" reflecting the kink shape: they decay on a scale proportional to the inverse kink width, which is given by $2d\equiv 2c_0/\omega_0$. Relevant examples are given in Table I. Result (8) omits all kink diffusion or lifetime effects and is derived in a Hamiltonian framework. Corresponding ideal gas results[13] for relativistic breather "particles" suggest central- *and* high-frequency components: for $X=c$ ($c\equiv\cos$)

$$S_{cc}^B(q,\omega;\omega_B;\text{central})=\frac{n_B(T;\omega_B)}{2\pi q}\frac{\omega_0^2}{\omega_B^2}\left[\frac{\omega_0^2}{\omega_B^2}-1\right]\times P\left[\frac{\omega}{q}\right]\gamma^{-1}\left[\frac{\omega}{q}\right]|f_c^B(q,\omega,\omega_B)|^2\ . \tag{10}$$

This central structure derives from the particlelike envelope of a breather of internal frequency ω_B. The internal oscillation itself yields the high-frequency response centered at[13]

$$\omega_B^m(q)\simeq\pm 2\omega_B(1-v_m^2/c_0^2)^{1/2}\pm v_m q\ , \tag{11}$$

where v_m is the velocity at which $\gamma^{-1}(v)P(v)$ is maximum; i.e., v_m also controls the central peak

TABLE I. Form factors.

$X(\phi)$	$\lvert f_X^K(Q)\rvert$
ϕ	$2\pi Q^{-1}[\cosh(\frac{1}{2}\pi Qd)]^{-1}$
$\sin\phi$	$4d(\frac{1}{2}\pi Qd)[\cosh(\frac{1}{2}\pi Qd)]^{-1}$
$\cos\phi$	$4d(\frac{1}{2}\pi Qd)\lvert\sinh(\frac{1}{2}\pi Qd)\rvert^{-1}$

splitting [Eq. (10)]. ω_B is restricted (classically[14]) to the continuous range $0\le\omega_B\le\omega_0$, but the upper frequency is limited by system size effects since breathers become arbitrarily extended as $\omega_B\to\omega_0$. The breather form factor (see Ref. 13) $f_c^B\to 0$ as $\omega_B\to 0$ *or* ω_0 and maximizes at $\omega_B^2=\frac{1}{2}\omega_0^2$. The breather densities are denoted by $n_B(\omega_B;T)$. The total response is the sum of contributions from all allowed breathers and is a competition of form factors, densities, and lifetimes. This competition is not well understood. We have argued previously[13,15] for a "preferred" breather with frequency $\bar{\omega}_B\simeq\omega_0/\sqrt{2}$, as suggested by the structure of the breather form factor. We expect that this is appropriate at high enought T. At low T, however, density effects may be expected to strongly favor low-energy (small amplitude, spatially extended) breathers. Contributions from such breathers can be described within conventional perturbation theory, as asserted elsewhere.[16] The corresponding power-series contributions from these *anharmonic* processes will compete with *harmonic* multiphonon expansion terms,[3,12,16] although these are interrelated and clear separation will be difficult unless large amplitude (nonperturbative) breathers dominate.

In Sec. III we demonstrate signatures of kinks, breathers, and phonons (including multiphonons). Our MD simulation is at the single temperature $k_BT=0.293E_K^{(0)}$, which is chosen because central peak splitting is apparent at this T but kink density is still low enough for a qualitative elementary mode interpretation. Splitting is not found[3] at $k_BT<(0.2-0.25)E_K^{(0)}$, and correspondingly we know[6,17] that asymptotic perturbation theories are valid in this T range for power series and exponential (kink) thermodynamic contributions. Concerning applications of SG to magnetic chains,[5,7,8] we should emphasize that this mapping is restricted (among other things) to *low*-velocity particlelike excitations.[5] Thus the onset of SG splitting is expected to coincide with the breakdown of the mapping—larger out-of-plane spin motions are energetically preferred. This is consistent with recent classical Heisenberg chain MD results,[11] although damping and quantum effects have yet to be assessed for real magnetic materials. It should be noted that the onset of splitting does not occur at the same T and q for all correlations and is strongly influenced by discreteness (Sec. III), so that the breakdown of a SG mapping may be similarly sensitive.

III. MOLECULAR DYNAMICS RESULTS AND INTERPRETATION

In this section we present our MD results for the dynamic correlation functions $S_{\phi\phi}$, S_{ss}, and S_{cc}, and interpret them in terms of linear phonon and multiphonon processes and kink and breather elementary modes. Kinks and breathers are both very evident in our data: in Fig. 1 we have shown examples of kink and *large*-amplitude breather dynamics projected from our data by a technique[3,15] (see Fig. 1 caption) which suppresses all small-amplitude fluctuations.

Breathers will not[13] contribute to odd ϕ correlations such as in $S_{\phi\phi}$ and S_{ss} ($s\equiv\sin$), and kink theory (8) is indeed rather successful *qualitatively*. For $S_{\phi\phi}$, Eq. (8) and Table I imply a *split* central peak with maximum at $\bar{\omega}_m=\bar{v}_m(\alpha)q$, where $\bar{v}_m(\alpha)$ is the maximum of $P(v)$ itself:

$$\bar{v}_m(\alpha)=\begin{cases}0\ , & \alpha>3\\ c_0(1-\alpha^2/9)^{1/2}\ , & \alpha<3\ .\end{cases}\tag{12}$$

MD results for the central structure in $S_{\phi\phi}(q,\omega)/\tilde{S}_{\phi\phi}(q)$ $[\tilde{S}_{\phi\phi}(q)\equiv\int(d\omega/2\pi)S_{\phi\phi}(q,\omega)]$ are shown in Fig. 2 and compared with the ideal gas prediction. We see that the orders of magnitude of intensities are consistent. However, with $\alpha=(0.293)^{-1}=3.41$ no splitting is predicted, whereas it is strongly evident (Fig. 2) in MD. Indeed a nonzero mean kink velocity $\bar{v}_m$ is apparent in Fig. 1 and consistent with the frequency location of the splitting. We propose that the basic kink mechanism is supported but that details depend strongly on both mode interactions and discrete lattice effects. Unfortunately, neither of these effects have been precisely assessed beyond linear perturbation order, which is generally insufficient for our purposes. Near-quantitative success in predicting the kink *density* can be achieved[17] by renormalizing $E_K^{(0)}$: At $k_BT=0.293E_K^{(0)}$ we use[17]

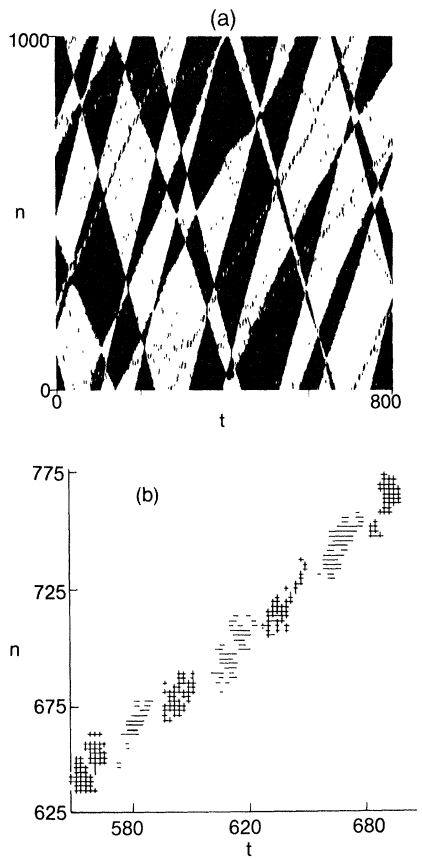

FIG. 1. (a) Space-time plot of the particle positions. Particle number n is plotted vertically and time is plotted horizontally. If, at time t the particle displacement $U_n(t)$ satisfies $-\pi < U_n(t) \leq \pi$, *or* if $U_n(t)$ minus an even integer (positive or negative) multiple of 2π is in this interval, then a white spot appears at the (t,n) position on the plot; otherwise a black spot appears. With this scheme, the boundaries between the large black and white regions are the midpoints of kinks and antikinks, and small bubbles of white in black regions or black in white regions are breathers with amplitude larger than π. (b) More detailed plot of the particle positions showing breather motion. If the particle displacement $U_n(t)$ satisfies $\pi < U_n(t) \leq 3\pi$ so that the nth particle is in the $(n+1)$st well, then a $+$ sign is put at the (t,n) position, and if it satisfies $-3\pi < U_n(t) \leq -\pi$ so that the nth particle is in the $(n-1)$st well, then a $-$ sign is put at the (t,n) position. This sequence of $+$ and $-$ signs showing the internal oscillation of a propagating breather appears in part (a) as the sequence of black bubbles for these (t,n) values.

$\alpha = 1.61$ (rather than 3.41). The result (see Fig. 2) is a notable improvement, but it is beyond this simple improvement to match *both* amplitude and location of the split peak (see the fits in Fig. 2).

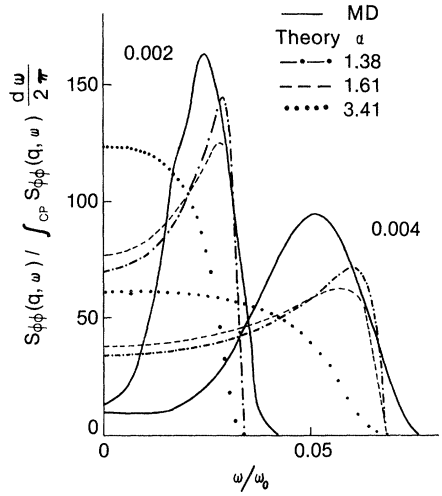

FIG. 2. Frequency spectra of the displacement-displacement correlation function [cf. Eq. (4)]. For each of the two wave vectors $\tilde{q} = 0.002$ and 0.004 the MD results are compared with ideal relativistic kink gas results calculated from Eqs. (8) and (9) and Table I for three different values of the parameter α. For each $\tilde{q}$ the curves are normalized to have the same total area. (For $\tilde{q} = 0.002$ the theory curve for $\alpha = 1.38$ and 1.61 coincide near the cutoff.)

We consider discrete lattice corrections to be equally serious. *Discreteness* becomes important for rapidly moving kinks where the continuous Lorentz symmetry breaks down, including the associated cutoff at $\omega = c_0 q$ [Eq. (8)]. The qualitative correction is to *increase* the effective continuum kink width d with increasing v/c_0 (or $\omega/c_0 q$). A consequence is the appearance of some weight for $\omega > c_0 q$, as observed by MD (Fig. 2). More importantly, the tendency to enhance weight at *smaller* ω/q (giving stronger and lower frequency splitting; Fig. 2) compared with the continuum theory can also be understood qualitatively from the enhancing effects[18] of discreteness on P and f_K. In a future publication we will analyze these corrections more fully by including numerical estimates of true kink widths and energies for arbitrary discreteness. We note that there are no *severe* central peak broadening mechanisms evident (from mode interactions beyond α renormalization).

$S_{ss}(q,\omega)$ is also well-described qualitatively by kink theory as far as its central peak structure is concerned. This can be expected since $S_{\phi\phi}$ and S_{ss} are directly related from the field equation of motion[3,13] (in a Hamiltonian framework):

$$\frac{S_{ss}(q,\omega)}{S_{\phi\phi}(q,\omega)}=\left[\left[\frac{\omega}{\omega_0}\right]^2-2\left[\frac{d}{a}\right]^2[1-\cos(qa)]\right]^2 \tag{13a}$$

$$\xrightarrow{qa\to 0}\left[qd\gamma^{-1}\left[\frac{\omega}{q}\right]\right]^4 . \tag{13b}$$

The continuum-limit result (13b) is exactly preserved within kink theory[11] but (13a) extends to all frequencies and predicts that at small q, the central intensity in S_{ss} is strongly depressed compared with $S_{\phi\phi}$, whereas a high-frequency component (from self-consistent phonon modes) is enhanced. Our MD results confirm this (see Fig. 3). A new feature should be emphasized—splitting of the central peak is observed, but only for sufficiently *large* q ($>q^*$). At $k_BT/E_K^{(0)}=0.293$, $\tilde{q}^*\simeq 0.008$, and splitting then develops strongly (Fig. 3). We can understand the appearance of q^* within kink phenomenology from (8) and Table I. In contrast to $S_{\phi\phi}$ *no* splitting is predicted from

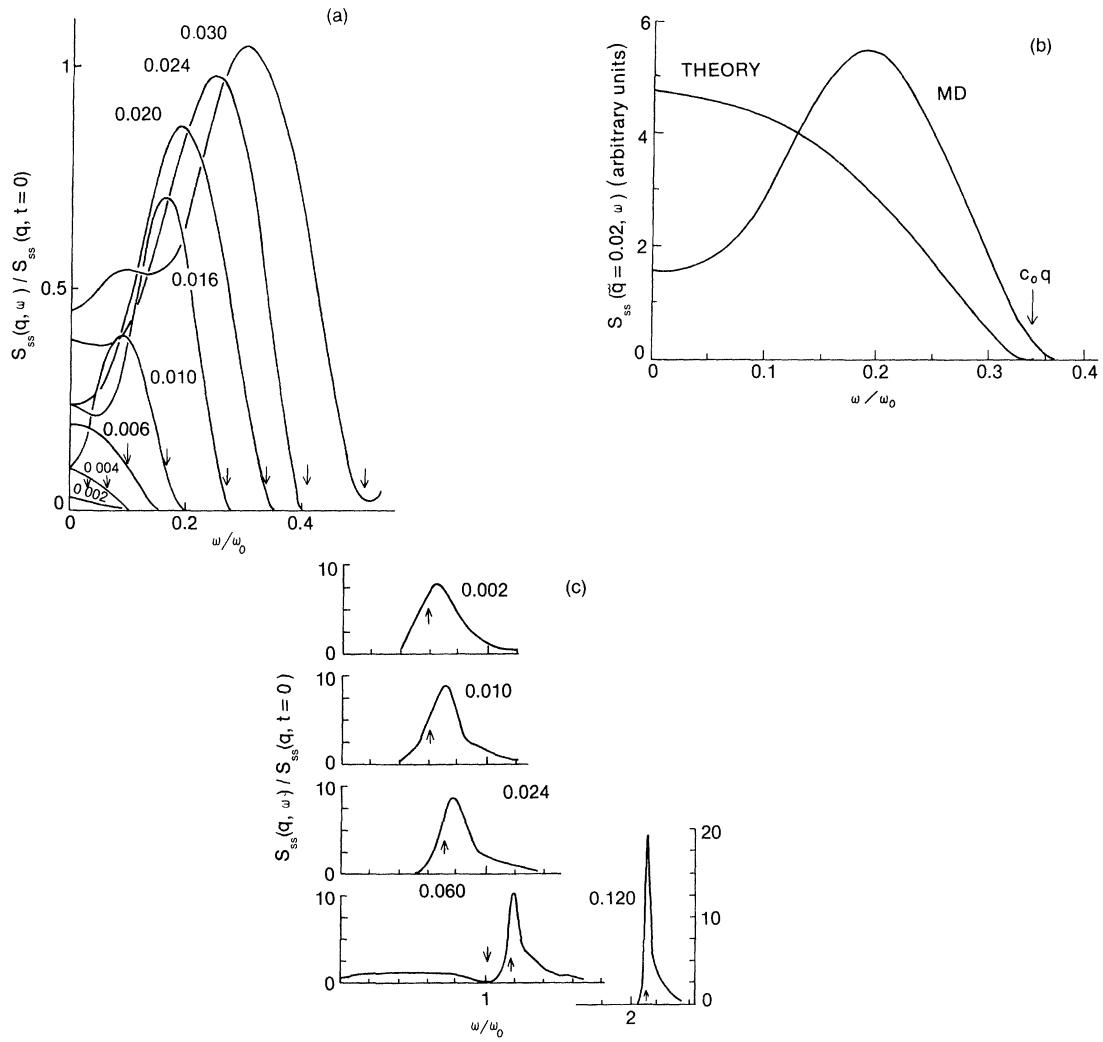

FIG. 3. Frequency spectra of the sine-sine correlation function [cf. Eq. (5)]. Each curve is labeled with the value of its wave vector $\tilde{q}$, and each is normalized by the initial value of its corresponding correlation function. (a) Low-frequency part of the frequency spectra. The arrows locate c_0q. (b) A typical comparison of MD results with ideal relativistic kink gas theory at $\tilde{q}=0.02$. The theory curve is calculated from Eqs. (8), (9), and Table I with $\alpha=1.61$. (c) High-frequency part of the frequency spectrum. The upward pointing arrows locate the self-consistent-harmonic phonon frequency. At $\tilde{q}=0.060$ the low-frequency part of the spectrum is also shown [continuing from part (a)], and the downward pointing arrow locates c_0q.

$P(v)$ and accompanying γ factors because these appear in the combination $\gamma^{-4}P(v)$. This predicts a monotonic decrease with ω/q for all α, but there is a competition with the structure factor which produces splitting for $q > q_0^*(\alpha)$ (the structure factor effect is weak for $S_{\phi\phi}$): a little algebra gives $\pi q_0^* d \tanh(\frac{1}{2}\pi q_0^* d) = 1+\alpha$. We find easily that q_0^* is always *larger* than the value q^* observed in MD. Indeed, even with $\alpha=0$ ($T=\infty$), $\tilde{q}_0^*$ is only 0.029. To be consistent with $S_{\phi\phi}$ we use $\alpha=1.61$ in Fig. 3(b) for comparison with MD; then $\tilde{q}_0^*=0.054$ to be compared with $\tilde{q}^* \simeq 0.008$ from MD. Again we can understand this discrepancy qualitatively as a discrete lattice effect[18] enhancing the competing terms in (8) more strongly as ω/q increases. Similarly a tail beyond $\omega=c_0 q$ is expected and observed[13] [Figs. 3(a) and 3(b)]. Notice [Fig. 3(a)] that resolvable splitting for S_{ss} is observed in MD for $\tilde{q} \lesssim 0.06$.

The more delicate nature of the splitting in S_{ss} makes it a better candidate for exposing the importance of corrections to ideal gas theory from both mode interactions (e.g., through α renormalization) *and* discreteness. To emphasize this we show in Fig. 3(b) a comparison of $S_{ss}(q,\omega)/\int S_{ss}(q,\omega;\text{central})d\omega/2\pi$ evaluated from MD and kink theory with α renormalized to 1.61. We use $\tilde{q}=0.02$, which we believe [see Fig. 6(a)] is in a region of quantitative validity for α-renormalized kink theory as far as $\int S_{ss}(\text{central})\, d\omega$ is concerned. Despite this successful description of the integrated weight, its distribution in frequency is poorly described [Fig. 3(b)]. We ascribe this to the greater role of form factors in determining splitting for S_{ss} (these are unaffected by α renormalization) than for $S_{\phi\phi}$. Note that any tendency towards relativistic splitting is beyond *linear* phonon-kink interaction theory[16] which also predicts a much too severe reduction in intensity at our T.

In Fig. 3(c) we have also shown the strongly weighted high-frequency structure in S_{ss}, whose location is quite well described by single-phonon response theory: self-consistent harmonic phonon theory[3] suggests a response at

$$\bar{\omega}(q)=[\omega_0^2\langle\cos\phi\rangle+(2C/M)(1-\cos qa)]^{1/2} ,$$

where $\langle\cos\phi\rangle$ is determined self-consistently, or (as we use here) evaluated from MD which gives $\langle\cos\phi\rangle \simeq 0.346$ at our T. The locations of $\bar{\omega}(q)$ are shown in Fig. 3(c); they are always slight underestimates. Higher-order multiphonon (see below) and anharmonic broadening mechanisms (including soliton-phonon interactions[16]) necessarily also contribute to S_{ss}. The asymmetry with additional weight on the high-frequency side of the single-phonon peaks [see Fig. 3(c)] is expected from these mechanisms. Similarly, we find evidence for such contributions to the *low*-frequency structure in S_{ss} at large q (see below).

We conclude that the structure in $S_{\phi\phi}$ and S_{ss} is basically well-described by kinks and phonons, although refined theories of discrete lattice effects and nonlinear mode interactions are still needed.

No such simple conclusions seem to be possible for S_{cc}, either for its central- or high-frequency structure observed in MD (see Fig. 4, and also Ref. 3). As we have explained elsewhere[13,15] (see also above), breather modes are expected to contribute strongly in both frequency ranges, whereas they cannot in $S_{\phi\phi}$ or S_{ss}. However, familiar multiphonon processes[3,12,16,19] are also clearly relevant and contributing in the same frequency regimes (there is no single-phonon response as in $S_{\phi\phi}$ and S_{ss}). At present it is not clear to what extent these various anharmonic effects are related (i.e., anharmonically broadened multiphonon processes versus extended breathers), although there are MD indications (below) that they can be distinguished as separate contributions at our temperature. No useful relationships can be learned from the equations of motion, as was the case for S_{ss}. Kinks should certainly make a central peak contribution to S_{cc}. According to ideal kink phonemenology [Eq. (8) and Table I],

$$\frac{S_{cc}^K(q,\omega)}{S_{ss}^K(q,\omega)}=\tanh^{-2}[\tfrac{1}{2}\pi q d\gamma^{-1}(\omega/q)] . \qquad (14)$$

Pure multiphonon theory[3,16,19] (i.e., without anharmonic broadening) yields a power series in $(k_B T/E_K^{(0)})$. The two-phonon term $[O(k_B T/E_K^{(0)})^2]$ comprises (i) a low-frequency continuous (difference) component which is essentially flat for $0 \le \omega \lesssim c_0 q$ with a square-root singularity at $\omega=c_0 q$. There is then a gap before the onset of a continuous high-frequency (sum) component again with a square-root singularity typical of one dimension (see below). The q dependences of breather, multiphonon, and kink contributions are distinguishable. From their form factors (Table I), kink structure-factor contributions decay characteristically for $\frac{1}{2}\pi q d \gtrsim 1$, i.e., $\tilde{q} \gtrsim 0.05$ with our parameter values. Breather contributions represent longer-ranged correlations—breathers all have at least twice a kink's spatial extent so that their form factors[13] [in (10)] generally produce decay at *smaller* q than for kinks. On the other hand, multipho-

non processes decay at *larger* characteristic q's (e.g., at $qd \sim 2$ for two-phonon terms) and with a Lorentzian rather than Gaussian dependence.

In Fig. 4 we have shown the MD data for low- and high-frequency structures in S_{cc}. At high frequency the noise level is high for small $\tilde{q}$ ($\lesssim 0.005$), but the broad two-peaked structures shown are within the numerical resolution. For $\tilde{q} \gtrsim 0.05$, weight in the lower-frequency structure is lost (or masked by weight in the higher-frequency

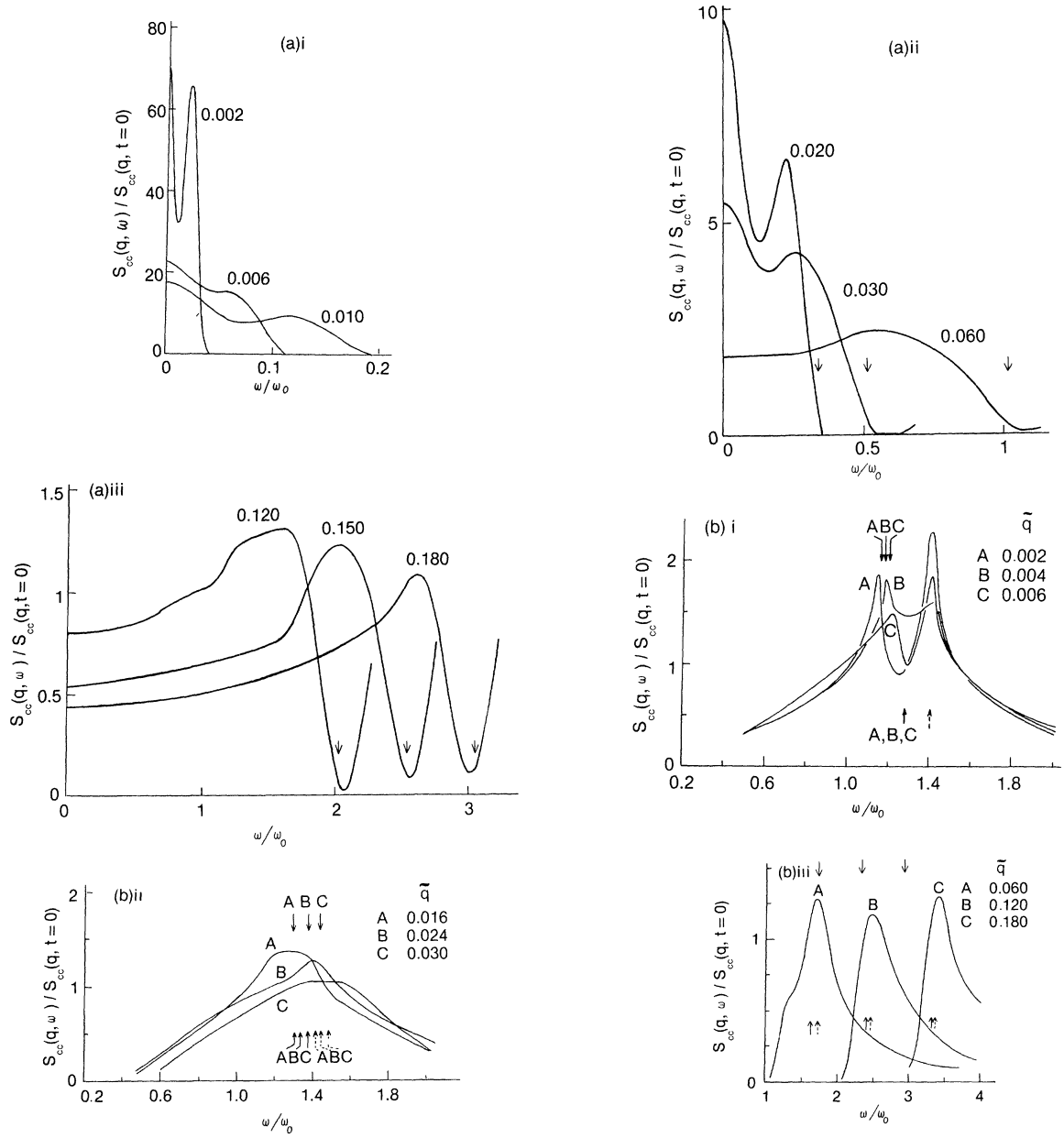

FIG. 4. Frequency spectra of the cosine-cosine correlation function [cf. Eq. (6)]. Each curve is labeled by the value of its wave vector $\tilde{q}$, and each is normalized by the initial value of its corresponding correlation function. (a) Low-frequency part of the frequency spectrum. The downward pointing arrows locate $c_0 q$. (b) The high-frequency part of the frequency spectrum. The downward pointing arrows locate $\bar{\omega}_B^m(q)$. The upward pointing solid arrows locate $\omega_2(q)$ as given by Eq. (15), with $\langle \cos\phi \rangle$ determined from the long-wavelength limit of $S_{ss}(q,\omega)$. If $\omega_0 \langle \cos\phi \rangle$ is fit to the high-frequency peak of $S_{cc}(q,\omega)$ at $\tilde{q}=0.002$ and that value used to compute $\omega_2(q)$ at other q values, the result is located at the upward pointing dashed arrow.

structure). For this q regime the two-phonon sum process fits increasingly well as q increases with a little smearing upon the predicted[3,16,19] *square-root* singularity at

$$\omega_2(q)=(4\omega_0^2+c_0^2q^2)^{1/2} =2\omega_0\langle\cos\phi\rangle^{1/2}[1+(\tfrac{1}{2}qd)^2/\langle\cos\phi\rangle]^{1/2} . \quad (15)$$

In writing (15) we have used the self-consistent phonon frequency as a reasonable approximation. An incipient square-root singularity becomes very plausible as q increases [see Fig. 4(b)iii]. Supposing that breather contributions are being comparatively lost with increasing q, it is also consistent that weight should be taken from lower frequencies first, since this is contributed from the more extended breathers whose form factors decay most rapidly with increasing q. The quadratic prediction for $\omega_2(q)$ [Eq. (15)] should be contrasted with the linear one for $\omega_B^m(q;\omega_B)$ from breather phenomenology [Eq. (11)]. It is hard to be definitive about the identification of the high-frequency peaks with our present data, and we do not believe that our understanding of breather or multiphonon structure-factor contributions and interrelations is sufficient to attempt an absolute comparison at this time. However, qualitatively, *one* interpretation is that the lower peak should be associated with a "dominant" breather,[13,15] i.e., dominant frequency $\bar{\omega}_B$ (and corresponding breather extent[13]). The selection of $\bar{\omega}_B$ is a combination of form factor [see below (11)], lifetime, and density effects which is not precisely known. Nevertheless we can impose a consistency requirement if we *suppose* that the location of the split *central* peak [Fig. 4(a)] is determined by the *same* breather type. In view of the anticipated discreteness and interaction effects (cf. discussions of S_{ss} and $S_{\phi\phi}$), we do not fit to the bare theory, Eq. (10), but rather take v_m directly from the MD data which gives $v_m/c_0=\omega_m/c_0q\simeq 0.59$, where we have taken an average ω_m for $q\leq 0.06$. Fitting the lower high-frequency peak to (11) for $\tilde{q}=0.002$ suggests $\bar{\omega}_B\simeq 0.71\omega_0$. This agrees surprisingly well with earlier expectations.[13,15] Note, however, that $\bar{\omega}_B$ is quite weakly preferred (see below). In Fig. 4 we have indicated the location of $\bar{\omega}_B^m(q)$ and $\omega_2(q)$ according to the above prescriptions. We observe that these coincide closely for much of our q range, and resolution of two distinct contributions in the MD data is not possible for intermediate q. Instead of $\langle\cos\phi\rangle^{1/2}$ in (15) we have used the actual long-wavelength phonon frequency observed in S_{ss} (Fig. 3). Even so, $\omega_2(q)$ is a slight underestimate of the observed peaks for all q. This could be a result of the broadening of (harmonic) two-phonon sum processes from the intrinsic anharmonicity in our system, and of higher-order multiphonon contributions which are also important (especially at our high T).

Within the above breather interpretation, we must conclude from Fig. 4 that $\bar{\omega}_B$ is only weakly preferred—significant weight is contributed from a wide range of frequencies around $\bar{\omega}_B$. We certainly expect that $\bar{\omega}_B\to\sim\omega_0$, as $T\to 0+$ because of breather density effects dominating form factor considerations (cf. Sec. II). In that case, the important breathers will be included in low-order anharmonic perturbation theories.[16] This approach has been advocated by Maki *et al.*,[20] emphasizing two-phonon *bound* states (*low*-energy breathers) as an alternative mechanism for the lower high-frequency peak in S_{cc}. Additional low-T ($\lesssim 0.2E_K^{(0)}$) MD simulations are highly desirable to understand relative breather contributions unambiguously.

Considering the central peak in S_{cc}, we recall that kinks [Eq. (3)], breathers [Eq. (10)], and two-phonon difference processes[3,12,16,19] all yield broad central peaks with cutoff $\omega=c_0q$ in the continuum limit. This agrees with the MD results (Fig. 4) except for the familiar tail for $\omega>c_0q$ from discreteness. For $\tilde{q}\lesssim 0.05$ there appear to be two central components—one with maximum at $\omega=0$ and one split to $\pm\omega_m\simeq\pm 0.59c_0q$. One proposal (above) associated the latter primarily with breathers. For $\tilde{q}\gtrsim 0.05$ the $\omega\simeq 0$ structure is lost and ω_m/c_0q increases with q (e.g., $\omega_m/c_0q\simeq 0.87$ for $\tilde{q}=0.18$). We argue below that kinks alone can substantially account for the integrated *central* intensity in S_{cc} for $\tilde{q}\lesssim 0.05$, so that a quite plausible alternative possibility at our T is that ω_m corresponds to the splitting appropriate to the *kink* central peak. Note, however, that bare kink theory [Eq. (8) and Table I] only predicts splitting for $k_BT>E_k^{(0)}$, a substantially higher T than for $S_{\phi\phi}$ [Eq. (12)]. Thus discrete lattice enhancement would have to be even more severe, dominating continuum form-factor influences and α renormalizations. Two-phonon difference processes yield a peak at $\omega_m\lesssim c_0q$—as stated earlier, the pure two-phonon difference process predicts a square-root singularity at $\omega=c_0q$ which is softened here by higher-order multiphonon effects, anharmonicity, and discreteness. For $\tilde{q}>>0.05$, this last mechanism fits neatly with our understanding (above) of the high-

frequency weight in S_{cc} in the same large q regime, where kinks (or breathers) contribute significantly less.

More detailed comments on the integrated weights $S_{cc}(q)$ and $S_{ss}(q)$ are in order. These contain less information than the detailed frequency structure but do support and quantify the interpretations we have made already. Results are shown in Fig. 5, where we contrast the total and partial (central) weights: Note that their q dependencies are quite distinct and we emphasize again that only the *total* intensities are rigorously available from transfer integral calculations.[6] In particular, the total intensities all decrease monotonically with increasing q (and agree with transfer integral results). By contrast, the central component of $S_{ss}(q)$ has a maximum at $\tilde{q} \simeq 0.07$ and is approximately proportional to q^2 as $q \to 0$, in qualitative agreement with kink theory predictions, even at our relatively elevated T. We also show in Fig. 6(a) the *absolute*[21] prediction of kink theory [Eq. (8)] with $\alpha = 1.61$. There is quantitative agreement for $\tilde{q} \lesssim 0.05$, where kink contributions are expected to be strongest, but there is significant additional weight at larger $\tilde{q}$ [see Fig. 6(a)]. This may be due to third (and higher)-order multiphonon contributions which should dominate those from kinks at large q. In addition, diffusive effects which are omitted in our ballistic kink theory become more important with increasing q, and discrete lattice effects will certainly move the location of the maximum in $S_{ss}(q)$. If α is not renormalized (i.e., $\alpha = 3.41$ is used), $S_{ss}(q)$ is overestimated by $\sim 50\%$ at small q.

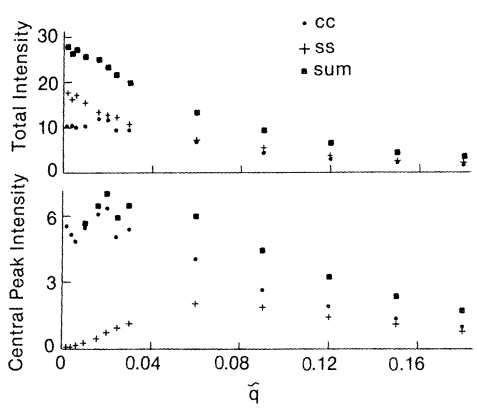

FIG. 5. Total intensities. The top part shows the integral over all frequencies for S_{cc}, S_{ss}, and their sum as a function of $\tilde{q}$. The bottom part shows the integral over the central peak alone. (For the three smallest q values, the points for the sum coincide with the S_{cc} points.)

To compare with MD results for $S_{cc}(q)$ we have computed [Figs. 6(b) and 6(c)] isolated contributions from kinks [integrating Eq. (8)] and from two-phonon difference processes[3,16,19]:

$$\int_0^{c_0 q} S_2(q,\omega)d\omega = \frac{d}{\pi}\left[\frac{k_B T}{E_K^{(0)}}\right]^2 [1+(\tfrac{1}{2}qd)^2]^{-1} . \tag{16}$$

Evidently, a very high proportion of the observed central weight in S_{cc} can be accounted for in this way. Kinks dominate for $\tilde{q} \lesssim 0.075$ and two-phonon processes for $\tilde{q} \gtrsim 0.075$. The small additional weight at large $\tilde{q}$ can be attributed to higher-order multiphonon processes (which decay more slowly with q) and anharmonicity. There appears little room for strong breather contributions at small $\tilde{q}$ (where they should be expected). This may be misleading: we should be wary of separating modes more than qualitatively at our T, especially where several nonlinearly-related contributions are competing and particularly for kinks and large-amplitude breathers. Certainly, the structure observed in $S_{cc}(q)$ at small $\tilde{q}$ (Fig. 5) is quite outside of isolated kink or two-phonon theory and in the anticipated breather regime. All of this points

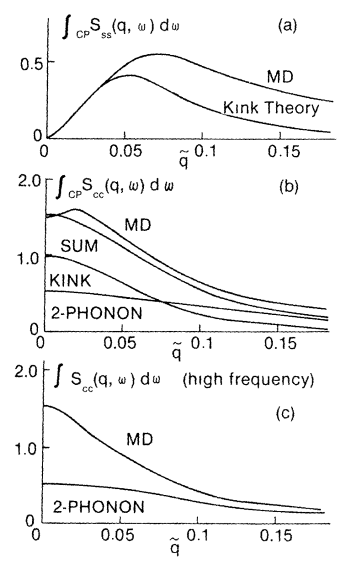

FIG. 6. Comparison of various contributions to spectral weight measured in *absolute* units (see Ref. 21). (a) Kink theory contribution compared to MD results for central peak intensity in S_{ss}. (b) Kink theory and two-phonon-difference contributions and their sum compared to MD results for central peak intensity in S_{cc}. (c) Two-phonon-sum contribution compared to MD results for high-frequency intensity in S_{cc}.

to the need for a better understanding of how these various processes are interrelated in a strongly nonlinear system. The separation will be much clearer (classically or quantum mechanically) at low T, where kinks and large-amplitude breathers will contribute much less weight because of their higher activation energies.

Fig. 6(c) compares the integrated *high*-frequency MD weight with the prediction of two-phonon sum processes—these give the *same* weight as Eq. (16).[3,16,19] The agreement is good for large q except for small additional weight from higher-order multiphonon contributions. However, as $\tilde{q}$ decreases below $\simeq 0.1$ there is an increasing additional weight [Fig. 6(c)] which must be accounted for, consistent with our discussion of frequency distributions. Indeed, pure two-phonon theory supplies less than 50% of the observed weight for $\tilde{q} \lesssim 0.05$. Although some anharmonic broadening will occur for multiphonon processes, it is tempting to attribute the additional weight to breather excitations as implied in Fig. 6(c)—dominated by preferred large-amplitude breathers or by extended, perturbative, two-bound-phonon breathers (see above). It is interesting to note that isolated ideal breather theory[13] predicts comparable high- and low-frequency weights in $S_{cc}(q)$. Clearly the large weight attributed to breathers at high frequency is *not* matched at low frequency according to our earlier discussion. This probably reemphasized the dangers of separating mode contributions too simplistically (since they are competing for central weight), but may also indicate the greater stability of breather internal degrees of freedom (responsible for high-frequency responses) compared with breather translation.

In Fig. 7 we have compared the percentages of component central- and high-frequency weights in $S_{cc}(q)+S_{ss}(q)$. Note the comparable contributions from both S_{cc} components at all q, and also large central contribution from S_{ss} for $\tilde{q} \gtrsim 0.05$.

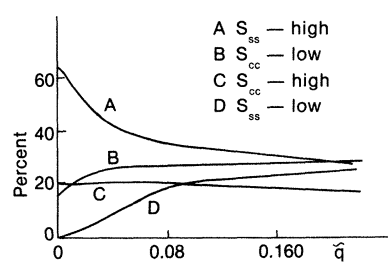

FIG. 7. Spectral weight in central peak and high-frequency components of $S_{ss}(q,\omega)$ and $S_{cc}(q,\omega)$ as a percentage of total weight in $S_{cc}+S_{ss}$.

IV. CONCLUDING COMMENTS

Our intention in Sec. III was to seek evidence for elementary contributions to correlation functions in the SG chain. In summary, our conclusions are the following.

(i) Central weight in S_{ss} is due to kinks for $\frac{1}{2}\pi qd \lesssim 1$. At larger q additional contributions from third (and higher)-order multiphonon processes seem likely.

(ii) The high-frequency weight in S_{ss} is predominantly a one-phonon response, with anharmonic broadening as well as contributions from higher-order multiphonon processes (especially important at larger q).

(iii) $S_{\phi\phi}$ and S_{ss} are exactly related [Eq. (13)] so that basic mechanisms and relative scales are understood. However, the origin of central-peak splitting within ideal kink theory is quite different. Also harmonic multiphonon contributions are not applicable to $S_{\phi\phi}$; thus the relationship (13) implies connections between anharmonic and multiphonon contributions.

(iv) The central- and high-frequency weight in S_{cc} at large q ($qd \gtrsim 2$) is predominantly the result of two-phonon processes, with small contributions from higher-order multiphonon processes.

(v) For $qd \lesssim 2$ other mechanisms become increasingly important to S_{cc} in addition to two-phonon (and higher-order) terms. At our T ($\simeq 0.3E_K/k_B$), kinks give a very large contribution to the central weight. The size of this contribution according to elementary kink gas theory may be misleading because of contributions anticipated from particlelike breather modes: at low $qd \lesssim 2/\pi$ anomalies do appear in the q dependence of the central weight (Fig. 5). In the same q range considerable additional weight (beyond two-phonon difference contributions) occurs at high frequency. This additional weight occurs over a broad frequency range but has a weak maximum at a frequency that scales with q differently from the two-phonon sum-onset frequency. The additional weight is probably due to anharmonicity in the form of bound phonons (breathers).

(vi) Comparable data at other (particularly lower) temperatures are needed for convincing identification of competing processes—kinks versus breathers in S_{cc} (central weight); intermediate-amplitude breathers [from structure-factor effects (3)] versus low-amplitude (low-order perturbational) breathers [supported by density enhancement (20)].

(vii) *Ideal* kink theory requires *strong* corrections due to mode-mode interactions *and* discrete lattice

effects. Neither of these are understood rigorously beyond low-order perturbation theory which is inadequate for $k_B T \gtrsim 0.2 E_K$ or moderate velocity kinks. Nevertheless, qualitative expectations are supported by MD results (see discussions of $S_{\phi\phi}$ and S_{ss}).

We conclude with a few remarks concerning application of SG theory to $CsNiF_3$.[5,7] We noted earlier that this application should be viewed very cautiously until more complete theoretical studies are available. Indeed it has been suggested[11] that a literal SG description does not apply at our T, a view with which we agree for the classical anisotropic Heisenberg model without external damping. Nevertheless, several features observed[7] in experiments on $CsNiF_3$ are in surprisingly good agreement with our results. Some general remarks are, therefore, in order.

(i) It is not expected[5,10,11] that resolvable central peak *splitting* would survive the perturbations on SG of real materials [damping, large out-of-plane fluctuations, or the discrete spin (all of which will affect kink, breather, and multiphonon processes differently)], but if it did, at small q, then ideal-gas fits would require distinct renormalizations as we have discussed.

(ii) Applications of kink-only theory may be quite good [especially for low and intermediate $\tilde{q} \lesssim 0.05$ (Ref. 22)] at moderately high T (which is where they have been mostly applied[7]). Contributions to S_{cc} (central) from multiphonon contributions only dominate at large q. Contributions to the high-frequency weight in $S_{ss}+S_{cc}$ from S_{cc} (i.e., in addition to the phonon contribution) are significant for all q (Fig. 7). These should be looked for even though they appear as a low-amplitude extended background. They should certainly appear at sufficiently low T (or high magnetic field)—corresponding responses have been observed[25] in TMMC.

(iii) Recent experiments[7] probing the central integrated intensity in the interesting q range $\tilde{q} \lesssim 0.05$, are consistent with the MD results reported here as we demonstrate in Fig. 8. This is, however, not a very sensitive test *except* at small q—$S_{ss}(q)+S_{cc}(q)$ has a maximum at $\tilde{q} \lesssim 0.04$ according to Fig. 5: This is largely driven by S_{ss} and so again is qualitatively within kink theory (and in good agreement with neutron scattering data[7]). However, consistent frequency distribution of weight would be the most clear-cut diagnostic. Similarly, regarding the absolute scale in Fig. 8, it is interesting to note that at $\tilde{q}=0.1$ the total central weight in spin-wave units[21] is 1.1. This compares favorably with the experimental observation[7] of $\simeq 1.0$, despite the possible breakdown of (e.g., frequency-dependent) SG predictions at this T[5,11]. T and q dependence of integrated weights are only weakly sensitive to, e.g., out-of-plane fluctuation perturbations.[11] It is not clear how sensitive the apparent structure (Fig. 5) in $S_{cc}(q)$ is to perturbations from SG (it is not a kink property).

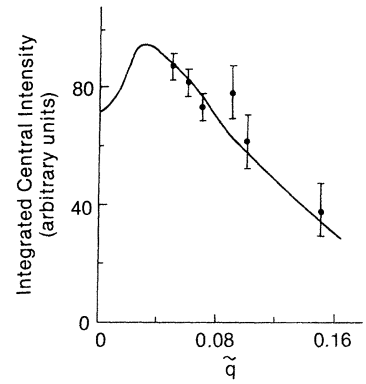

FIG. 8. Integrated central peak intensity in $S_{ss}+S_{cc}$ from MD calculations compared to experimental results on $CsNiF_3$ taken from Ref. 7. Results were *fitted* at smallest $\tilde{q}$ value, but absolute intensity comparisons agree to within 10% (see also Sec. IV).

(iv) The weight in out-of-easy-plane fluctuations (linear theory[5]) is much less (factor of ~ 30 with our parameters) than in S_{cc}, so careful experiments would be needed to distinguish it.

(v) A very serious open question for $CsNiF_3$ is the validity of a SG field theory description for an $S=1$ magnetic chain dynamics. If it is argued that most weight in the classical (or quantum-field theory) SG model correlation functions can be attributed to single-phonon (magnon) or two-phonon sum-difference processes,[12] then we expect that they can be satisfactorily reconciled with equivalent processes[12] in the $S=1$ chain simply by rescaling effective Hamiltonian parameters, as is familiar for the linear magnon modes already.[23] If, however, strongly nonlinear modes also contribute importantly to the SG correlations (as implied here for certain regions of T, ω, and q space), then much less clear questions must be faced, especially for dynamics—namely, the nonlinear analogs (if any) in an $S=1$ chain and the importance of out-of-easy-plane fluctuations upon them.

In a future paper we will present corresponding MD results for correlations of $\sin\frac{1}{2}\phi$ and of $\cos\frac{1}{2}\phi$. These are experimentally relevant (although at lower T) to the antiferromagnet TMMC (Ref. 8)

and are theoretically interesting as largely *kink*-sensitive functions[6,8,24] at small q. The relevant kink phenomenologies must be distinguished, however, from the ones used above, where, e.g., kink densities directly controlled a central peak *intensity*. In the kink-sensitive function cases, kinks are responsible for a broadened Bragg central peak and their density controls the *broadening*. Appropriate kink phenomenology is then akin to that required for ϕ correlations in the ϕ-four model,[5,26] but contrasts will be drawn because of the strong role of quasibreathers in ϕ^4 which affect kink dynamics much more severely than in SG. In particular, central peak splitting in ϕ^4 in lost.[3,27] We have also obtained MD results for a SG chain with a random array of impurities.[19,28] Dynamic responses for this system will be presented elsewhere and compared with the results and mode interpretations for the pure chain.

ACKNOWLEDGMENTS

The part of this work carried out at Wake Forest University was supported by a Grant from the Research Corporation. One of us (A.R.B.) acknowledges the support of the USDOE.

---

[1]D. Beeman, J. Comput. Phys. 20, 130 (1976).

[2]W. C. Kerr, Phys. Rev. B 19, 5773 (1979).

[3]T. Schneider and E. Stoll, Phys. Rev. B 23, 4631 (1981).

[4]For example, K. Kawasaki, Prog. Theor. Phys. 55, 2029 (1976); K. M. Leung, and D. L. Huber, Solid State Commun. 32, 127 (1979); N. Theodorakopoulos, in *Ordering in Strongly Fluctuating Condensed Matter Systems,* edited by T. Riste (Plenum, New York, 1980).

[5]H. J. Mikeska, J. Phys. C 11, L29 (1978); J. Appl. Phys. 52, 1950 (1981).

[6]For example, P. Riseborough and S. E. Trullinger, Phys. Rev. B 22, 4389 (1980); D. W. Hone and K. M. Leung, *ibid.* 22, 5308 (1980); T. Schneider and E. Stoll, Phys. Rev. B 22, 5317 (1980); A. R. Bishop, J. Phys. A 14, 883 (1981).

[7]J. K. Kjems and M. Steiner, Phys. Rev. Lett. 41, 1137 (1978); K. Kakurai, J. K. Kjems, and M. Steiner, in *Ordering in Strongly Fluctuating Condensed Matter Systems,* edited by T. Riste (Plenum, New York, 1980); M. Steiner, in *Physics in One-Dimension,* edited by J. Bernasconi and T. Schneider (Springer, Heidelberg, New York, 1981); and private communications.

[8]J. P. Boucher, L. P. Regnault, J. Rossat-Mignod, J. P. Renard, J. Bouillot, and W. G. Stirling, Solid State Commun. 33, 171 (1980); 33, 311 (1979); J. Appl. Phys. 52, 1956 (1981).

[9]H. J. Mikeska and E. Patzak, Z. Phys. B 26, 253 (1977); K. Maki and H. J. Takayama, Phys. Rev. B 20, 5002 (1979); A. R. Bishop, J. Phys. C 13, L67 (1980).

[10]A. R. Bishop, Z. Phys. B 37, 357 (1980).

[11]J. M. Loveluck, T. Schneider, E. Stoll, and H. R. Jauslin, Phys. Rev. Lett. 45, 1505 (1980).

[12]G. Reiter, J. Appl. Phys. 52, 1961 (1981); Phys. Rev. Lett. 46, 202 (1981); 46, 518 (1981).

[13]A. R. Bishop, J. Phys. A 14, 1417 (1981). Notice that the right-hand side of Eq. (13a) is zero at $\omega=2(d/a)\,|\sin(qa/2)|$, implying that $S_{ss}(q,\omega)$ is zero at this frequency. The MD results for $S_{ss}(q,\omega)$ in Fig. 3(a) show a sharp cutoff near this ω, but are not precisely zero due to numerical errors. This failure of the data for $S_{ss}(q,\omega)$ to vanish at this point means that Eq. (13a) is not useful for obtaining $S_{\phi\phi}(q,\omega)$ directly from the $S_{ss}(q,\omega)$ data.

[14]Note that upon quantization, the SG breather spectrum becomes discretized such that the lowest energy (most extended) breather coincides with the single "elementary" quantum (the phonon or magnon). Inclusion of this low-energy discretization of the spectrum is essential in the construction of a statistical theory (see, e.g., Ref. 20).

[15]E. Stoll, T. Schneider, and A. R. Bishop, Phys. Rev. Lett. 42, 937 (1979).

[16]E. Allroth and H. J. Mikeska, J. Phys. C 13, L725 (1980); cf. P. S. Sahni and G. F. Mazenko, Phys. Rev. B 20, 4674 (1979).

[17]A. R. Bishop, Solid State Commun. 30, 37 (1979).

[18]P. Riseborough, D. L. Mills, and S. E. Trullinger, J. Phys. C 14, 1109 (1981).

[19]D. Baeriswyl and A. R. Bishop, J. Phys. C 13, 1403 (1980); D. Baeriswyl, A. R. Bishop, and W. C. Kerr (unpublished).

[20]Cf. K. Maki, in *Physics in One-Dimension,* edited by J. Bernasconi and T. Schneider (Springer, Heidelberg, New York, 1981).

[21]For experimental and theoretical comparison with other works, we use here the *absolute* units of scattering intensity advocated in Ref. 16, viz., the zero-temperature, long-wavelength one-spin wave intensity which with our parameters becomes $\simeq 0.052d$, with $d \simeq 5.406a$.

[22]The characteristic q values quoted throughout the paper are determined by the scale d^{-1}. Consequently these values are sensitive to the magnetic field strength in, for instance, $CsNiF_3$. Having this example in mind, we have assumed a field of 5 kG

(cf. Ref. 7).
[23]See, e.g., M. Steiner, J. Villain, and C. G. Windsor, Adv. Phys. 25, 87 (1976).
[24]For example, K. M. Leung, D. W. Hone, D. L. Mills, P. S. Riseborough, and S. E. Trullinger, Phys. Rev. B 21, 4017 (1980).
[25]G. Reiter, private communications.
[26]For example, J. A. Krumhansl and J. R. Schrieffer, Phys. Rev. B 11, 3535 (1975).
[27]T. R. Koehler (unpublished).
[28]W. C. Kerr, D. Baeriswyl, A. R. Bishop, and S. N. Kerr, Bull. Am. Phys. Soc. 25, 239 (1980).